

Ionic conductivity ageing behaviour of 10 mol.% Sc_2O_3 –1 mol.% CeO_2 – ZrO_2 ceramics

Shobit Omar · Nikolaos Bonanos

Received: 18 March 2010 / Accepted: 15 June 2010 / Published online: 29 June 2010
© Springer Science+Business Media, LLC 2010

Abstract The long-term ionic conductivity behaviour of samples of zirconia co-doped with 10 mol.% of Sc_2O_3 and 1 mol.% CeO_2 is evaluated in oxidizing and reducing atmospheres at 600 °C. After 3,000 h, the sample kept in reducing atmospheres exhibits 20% loss in the ionic conductivity, while the sample kept in air shows 6% degradation. No phase transitions were observed in the samples after both the ageing studies. The main contribution towards the loss in the ionic conductivity of the sample kept in air comes from grain boundaries; however, for the sample aged in reducing conditions, both grain and grain boundary contribute similarly towards the increase in the total resistivity. This is tentatively explained by the reduction of Ce^{4+} cations, dissolved in the fluorite lattice of ZrO_2 .

Introduction

Highly oxygen ion conductive Sc-doped zirconia (ScSZ) electrolyte materials have opened up the prospects for the development of intermediate temperature solid oxide fuel cells [1]. At 850 °C, the ionic conductivity of zirconia doped with 11 mol.% Sc_2O_3 (11ScSZ) is nearly 1.5 times higher than the state-of-the-art yttria stabilized zirconia [2]. However, below 600 °C, the highly conductive cubic phase in 11ScSZ undergoes a phase transition to rhombohedral phase (β -phase) [3]. This phase transformation is detrimental to both the ionic conductivity and the mechanical

integrity of the electrolyte. The appearance of the low temperature poor conducting β -phase has been described on the basis of oxygen vacancy ordering [4]. The ordering also occurs over time at higher temperatures resulting in a phase transition from cubic to β -phase, which degrades the ionic conductivity [5]. Previously, it has been shown that oxygen vacancy ordering can be suppressed by substituting 1 mol.% of Sc_2O_3 for other oxides such as Gd_2O_3 [6], Y_2O_3 [7], Bi_2O_3 [8], CeO_2 [4]. Arachi et al. [4] studied the structural behaviour of zirconia co-doped with Ce^{4+} and Sc^{3+} . It is reported that the co-doped compositions no longer exhibits an unfavourable phase transition at any temperature. Further, Lee et al. [9] tested the long-term stability of zirconia doped with 1 mol.% CeO_2 and 10 mol.% Sc_2O_3 (1Ce10ScSZ) at 1000 °C for 600 h in air. The stable ionic conductivity value of 1Ce10ScSZ indicates no phase transition, or other effects such as grain boundary segregation and defect ordering with time. Nevertheless, the tendency of Ce^{4+} to transform to Ce^{3+} under the low-partial pressure of oxygen and at high temperature may affect the ionic conductivity stability of 1Ce10ScSZ. The high-temperature performance of this material in reducing atmospheres over time still needs to be investigated. The present work is a study of the ionic conductivity ageing in both reducing and oxidizing atmospheres at 600 °C.

Experimental

Polycrystalline samples of 1Ce10ScSZ were synthesized via conventional solid-state reaction method, starting from stoichiometric mixtures of 10ScSZ and CeO_2 . The starting powders were heated to 900 °C for 1 h in order to compensate for the loss on ignition. Accordingly, the

S. Omar (✉) · N. Bonanos
Fuel Cells and Solid State Chemistry Division, Risø National
Laboratory for Sustainable Energy, Technical University
of Denmark—DTU, Roskilde 4000, Denmark
e-mail: shobit.omar@risoe.dk

stoichiometric amount of powders were weighed and ball milled in ethanol for 24 h. The ball milled slurry was then dried at 100 °C. The agglomerated powders were ground using mortar and pestle and then uniaxially pressed into pellets (12 mm in diameter and 2 mm thick) and bars ($5 \times 5 \times 10$ mm³). This was followed by the isostatic pressing with 250 MPa for 1 min. The green ceramic pellets were then sintered in air at 1,500 °C for 6 h. The relative geometrical density of the sintered ceramic samples was calculated to be 96% of the theoretical density or above.

Ionic conductivity ageing studies were performed on sintered ceramic samples of 1Ce10ScSZ using impedance spectroscopy at 600 °C. For the impedance measurement, Pt paste was brushed onto both faces of the pellet to serve as the electrode. The pellets were then co-fired at 1,200 °C for 1 h. The impedance of the sample was measured in situ using Solartron 1260 over the frequency range of 100 Hz to 2 MHz with an applied potential of 100 mV. In the present study, samples were kept in air and in a gas mixture of 9% H₂, 1% H₂O and 90% N₂ (composition given in vol.-%), and at the same time, the impedance of the samples was measured for a time period of 3,000 h, at regular intervals. The partial pressure of oxygen gas was determined using a Nernst sensor, and was measured to be 5.07×10^{-26} atmospheres in the wet mixture of H₂ and N₂. The flow rate of the gases was maintained at 120–130 cm³/min.

In order to study any phase transformation after the ageing period, X-ray diffraction (XRD) patterns were collected with Bruker D8 diffractometer (using the incident CuK α radiation) on both the aged and unaged sintered samples of 1Ce10ScSZ. Lattice parameter was estimated using Nelson–Riley extrapolation method [10]. The scanning electron microscopy was performed using Hitachi TM-1000 in a backscattered mode with the accelerating voltage of 15 kV.

Results and discussion

XRD

Figure 1 shows the XRD profiles of an unaged and aged samples of 1Ce10ScSZ collected at room temperature. The unaged sample exhibit cubic fluorite structure with the lattice parameter of 5.0956(1) Å. It confirms that the addition of 1 mol.% CeO₂ in 10ScSZ stabilizes the high-temperature cubic phase to room temperature. Both the aged samples exhibit similar XRD pattern (as the unaged sample), which indicates that no phase transition had taken place even after annealing for 3,000 h at 600 °C. The two extra peaks present in the XRD pattern of the sample aged in reducing conditions, are due to Pt electrodes. In the inset of Fig. 1, (220) peak of all the samples is shown. The peak

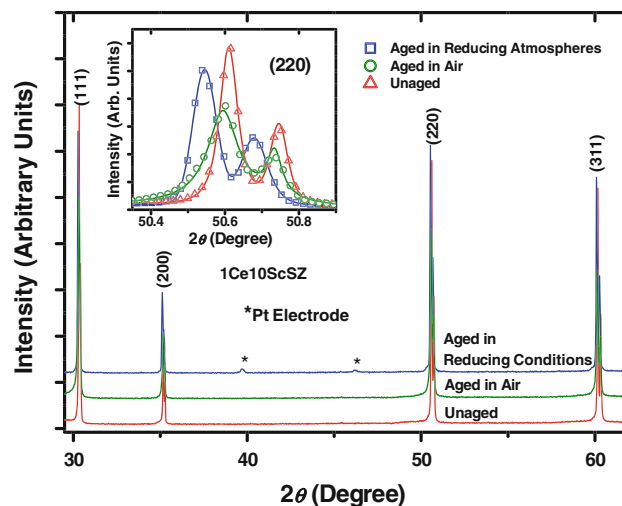


Fig. 1 XRD profiles of aged and unaged samples of 1Ce10ScSZ. In the inset, (220) peak of all the samples is shown. The dots are the experimental data while the line is the symmetric Pearson VII peak fit

position in the sample aged in reducing conditions shifts towards lower 2θ position, while the sample aged in air exhibits only slight peak shift when compared with the unaged sample. The peak shift towards lower 2θ position indicates the crystal lattice expansion of the aged samples. The lattice parameter of the samples aged in air and in reducing atmospheres is estimated to be 5.0963(1) and 5.0975(3) Å, respectively. An increase in the lattice parameter of the sample aged in reducing conditions can be attributed to the reduction of Ce⁴⁺ cations to Ce³⁺, which in turn further expands the crystal lattice ($r_{\text{Ce,VIII}}^{3+} = 0.1143$ Å, $r_{\text{Ce,VII}}^{4+} = 0.0970$ Å). Further, the reason for the slight lattice expansion in the sample aged in air is not known. Nevertheless, this may be associated with the inhomogeneous distribution of Ce⁴⁺ cations in the zirconia lattice or the elastic strain formed during the high-temperature ageing process.

Microstructure

Figure 2 shows the backscattered micrograph of the sintered unaged sample of 1Ce10ScSZ taken at the accelerating voltage of 15 kV. The sample is densely sintered with a few isolated residual pores. This is consistent with the measured geometrical density of the sintered sample. The average grain size was found to be 6–8 µm. Figure 2 also shows the optical images of the unaged and aged samples of 1Ce10ScSZ. The grey colour surface of both the aged samples is the Pt electrode. The colour of the unaged sample is similar to that of the sample aged in air, while after ageing in reducing conditions, the sample colour changed from white to dark orange. This again suggests the reduction of 1 mol.% Ce⁴⁺ cations which are dissolved in the fluorite lattice of ZrO₂.

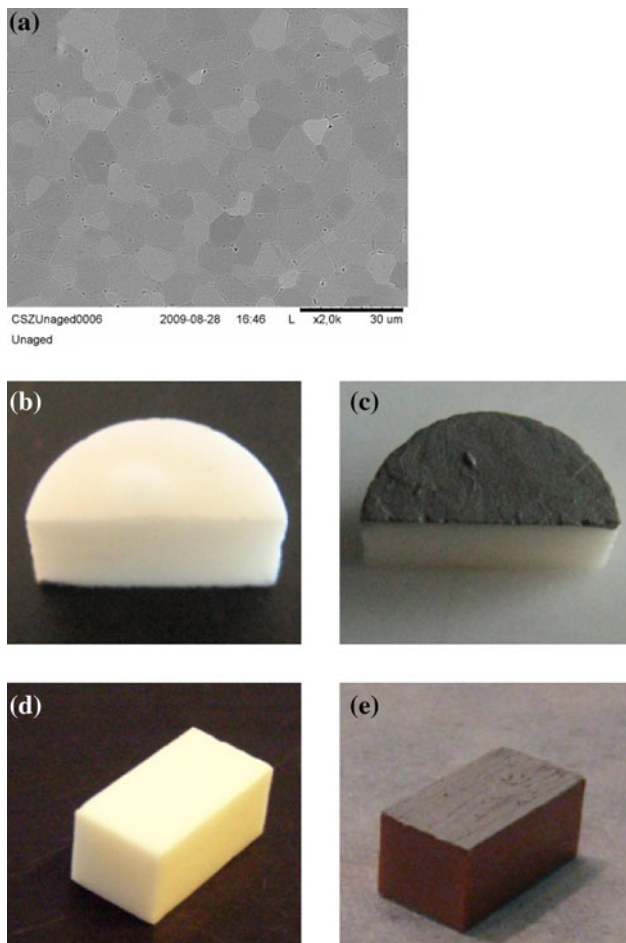


Fig. 2 Backscattered electron micrograph of the sintered thermally etched surface of an unaged 1Ce10ScSZ (a), and optical images of the before (b) and (d) and after ageing of 1Ce10ScSZ samples in air (c) and in reducing conditions (e)

Ionic conductivity

The conductivity of the unaged sample of 1Ce10ScSZ was measured as a function of temperature. The activation energy was calculated from the gradient of the quadratic fit of the Arrhenius plot. The ionic conductivity of the unaged sample of 1Ce10ScSZ at 600 °C was measured to be 11.6 mS cm⁻¹ with the activation energy of 1.091 eV at 600 °C in air. For ageing studies, unaged samples were placed in a different furnace which had around 4–5 °C offset from 600 °C. Although, this temperature offset leads to a difference in the initial ionic conductivity of the sample, the relative degradation in the total ionic conductivity can still be measured with confidence. The initial conductivity of the sample aged in air and in reducing conditions at 600 °C are 12.7 and 11.1 mS cm⁻¹, respectively. Figure 3 shows the degradation in the normalized total ionic conductivity of the sample kept in air and in a gas mixture of 9% H₂, 1% H₂O and 90% N₂ at 600 °C. For

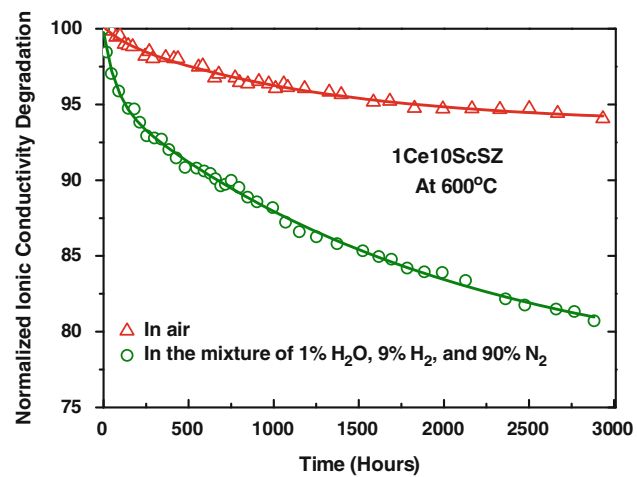


Fig. 3 Normalized ionic conductivity of 1Ce10ScSZ aged in air and in reducing conditions at 600 °C

the purpose of extrapolating the conductivity value at longer times, the experimental data were fitted using the second-order exponential decay function. The function itself does not carry any physical significance, but is employed as it gave reasonably good fit over the whole range of ageing times. Following is the fitted relationship in both the conditions,

In air,

$$\sigma_{\text{Normalized}} = 93.71 + 0.67 \times \exp(-t/108.94) + 5.74 \times \exp(-t/1232.01). \quad (1)$$

In reducing conditions,

$$\sigma_{\text{Normalized}} = 76.50 + 4.38 \times \exp(-t/74.26) + 18.86 \times \exp(-t/2002.04), \quad (2)$$

where $\sigma_{\text{Normalized}}$ is the ionic conductivity normalized to 100 and t is the annealing time.

The sample annealed in reducing conditions exhibits higher conductivity degradation than the sample kept in air. After 3,000 h, the samples placed in air and in reducing conditions at 600 °C show 5.8 and 20% loss in the ionic conductivity, respectively. On extrapolating the fitted curves (Eqs. 1–2), the ionic conductivity of the samples placed in air and in reducing conditions may fall by 93.8 and 78%, respectively, of the initial total conductivity after 5,000 h. For the first 1,000 h, the degradation rate is higher than in the subsequent 2,000 h; thereafter, ionic conductivity degrades linearly as a function of time and this applies to both samples. Experimentally, after 1,000 h, the degradation rate in the ionic conductivity for the samples placed in air and in reducing conditions is 1.0 and 3.8% per 1,000 h, respectively. The difference in the degradation rates can be attributed to the reduction of Ce⁴⁺ cations to Ce³⁺, which creates an additional elastic strain in the crystal lattice.

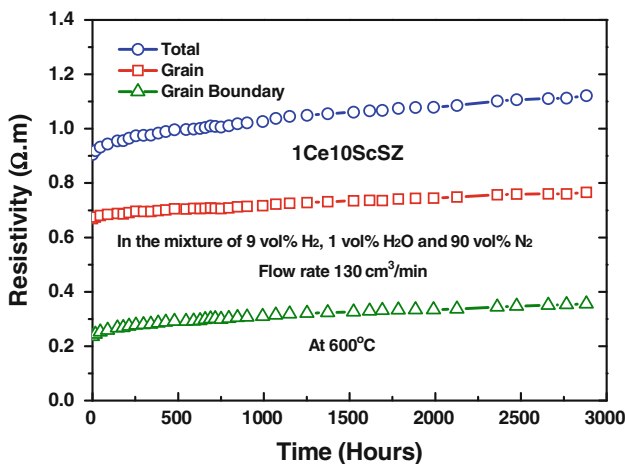


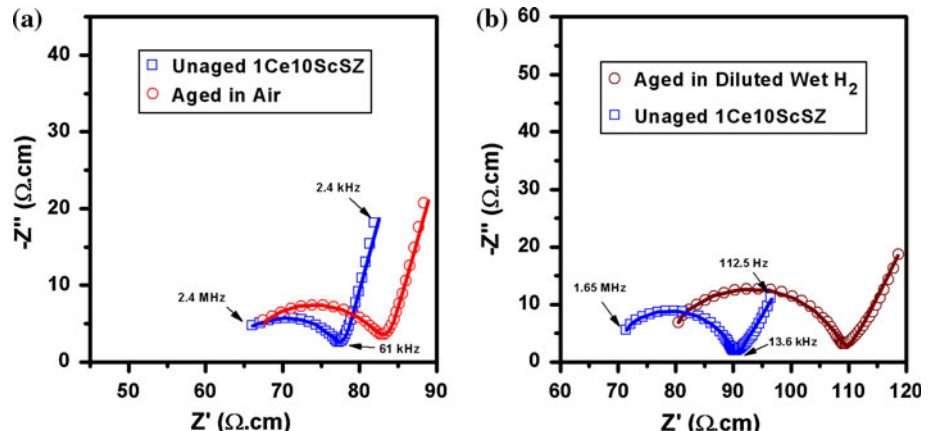
Fig. 4 Grain and grain boundary contribution towards the total resistivity of the 1Ce10ScSZ sample kept in reducing environment

Figure 4 shows the grain and grain boundary components of the total ionic resistivity with time of the sample kept in reducing environment. Due to the additive nature of the resistivity contributions, plotting resistivity instead of conductivity in Fig. 4 makes it easier to identify the individual contribution of grain and grain boundary. The increase in the grain boundary resistivity component is slightly higher than that of grain. The grain boundary resistivity increment is 54% of the rise in the total resistivity after ageing for 3,000 h at 600 °C. Figure 5 shows the impedance spectrum of the unaged sample and samples aged in (a) air and (b) diluted wet hydrogen at 600 °C. The high frequency semicircle due to the intra-grain polarization is not observed in all the curves. The intermediate semicircle is due to the grain boundary polarization and is confirmed by its capacitance value ($\sim 1.9 \times 10^{-8}$ F/cm). The grain and the grain boundary resistance was calculated by fitting the observed impedance spectra with the analog equivalent circuit having a resistor and two parallel pair of resistor-constant phase element (R-CPE) connected in series. An external inductor was also used in the equivalent

circuit, while fitting the impedance data. Figure 5a and b are in different scaling because the measured initial resistivity of both the samples were different. The difference in the impedance of both the unaged samples is associated with the temperature offset in the furnaces mentioned earlier. From the impedance plot, it can be seen that in both the unaged samples, the grain boundary contribution towards the total resistivity is lower than that of grain. After ageing, the grain boundary polarization semicircle (in the impedance plot) in both the samples becomes larger than in the unaged sample. This indicates the increase in the grain boundary resistance during the ageing process. However, in the sample aged in the diluted wet hydrogen, there is a large shift in the grain boundary polarization semicircle towards the higher real impedance (Z') value, compared to the sample aged in air. This shift is associated with the increase in the grain resistance in the sample. The sample aged in reducing conditions exhibits higher increase in grain resistivity than the sample aged in air. The % increase in the grain resistivity to the total increase in the resistivity of the sample aged in diluted wet hydrogen is $\sim 46\%$, which is 15% higher than the sample aged in air. Although, the total resistivity rise in the sample aged in reducing conditions is 4.4 times higher than the sample aged in air, the ratio between the grain boundary and grain resistivity increase decline from the sample aged in air (~ 2.4) to the sample aged in reducing conditions (~ 1.2). This shows that in the reducing conditions, the grain resistivity also increases significantly and contributes towards the increase in the total resistivity. The enhancement in the grain resistance during the ageing in reducing atmosphere is associated with the reduction of Ce^{4+} cations to Ce^{3+} (as evident from the optical image), which creates an extra lattice strain in the material. We suppose that this lattice strain hinders the migration of oxygen vacancies, lowering the ionic conductivity of the material.

The rise in the grain boundary resistivity in the sample after aged in reducing conditions is 3.3 times higher than in

Fig. 5 Impedance spectra of 1Ce10ScSZ sample before and after ageing in **a** air and **b** reducing conditions at 600 °C for 3,000 h



the sample aged in air. The increase in the grain boundary resistance in the sample aged in reducing conditions can be explained by the slow diffusion of Ce^{3+} from the grain interior towards the grain boundaries. These cations form the blocking layer for the oxygen vacancy to jump across the grain boundaries. Transmission electron microscopy to test this hypothesis is in progress and will be reported in a future communication.

Conclusions

The long-term ionic conductivity ageing studies were performed on 1Ce10ScSZ in both oxidizing and reducing atmospheres at 600 °C. After 3000 h, sample kept in reducing conditions shows 20% loss in ionic conductivity while the sample placed in air exhibits 6% loss in total ionic conductivity. The change in the colour of the sample placed in reducing conditions indicates reduction of Ce^{4+} cations. For the sample aged in air, the main contribution towards the loss in the total ionic conductivity comes from the increase in the grain boundary resistivity. However, for the sample aged in reducing conditions, both the grain and the grain boundary contribute similarly towards the total resistivity. The increase in the grain resistivity in the sample aged in reducing condition is associated with the

reduction of Ce^{4+} cations to Ce^{3+} , which creates an additional elastic lattice strain in the material.

Acknowledgements Waqas Bin Najib, formerly Ph. D. student at this Division, is thanked for preparation of samples and initiation of the ageing studies. This work has been supported by the EU, within the integrated project SOFC600, Demonstration of SOFC stack technology for operation at 600 °C, Project Ref. 20089.

References

1. Badwal SPS, Ciacchi FT, Milosevic D (2000) Solid State Ion 136:91
2. Badwal SPS, Ciacchi FT (2000) Ionics 6:1
3. Fujimori H, Yashima M, Kakihana M, Yoshimura M (2002) J Appl Phys 91:6493
4. Arachi Y, Asai T, Yamamoto O, Takeda Y, Imanishi N, Kawate K, Tamakoshi C (2001) J Electrochem Soc 148:A520
5. Haering C, Roosen A, Schichl H, Schnoller M (2005) Solid State Ion 176:261
6. Yamamura H, Matsusita T, Nishino H, Kakinuma K (2002) J Mater Sci Mater Electron 13:57
7. Yamamura H, Utsunomiya N, Mori T, Atake T (1998) Solid State Ion 107:185
8. Hirano M, Oda T, Ukai K, Mizutani Y (2003) Solid State Ion 158:215
9. Lee DS, Kim WS, Choi SH, Kim J, Lee HW, Lee JH (2005) Solid State Ion 176:33
10. Nelson JB, Riley DP (1945) Proc Phys Soc Lond 57:160–177